

Atomic and Molecular Photoionization Studies using Synchrotron Radiation

J. B. WEST

*Research Institute for Scientific Measurements, Tohoku University**

Measurements made at the Daresbury SRS on a selection of atoms and small molecules are presented in this review, where the emphasis is on the effects of electron correlations and the means of quantifying them by focussing on resonant structure in the photoionization continuum. The use of the techniques of angle resolved electron spectrometry, fluorescence polarization analysis and merged ion beam spectrometry to highlight these effects is discussed, as well their application in providing fundamental data on the photoionization process. The results presented have been chosen not only to give an indication of our present state of understanding of this field, but also to show how it is likely to develop in the future, in the context of the newly established coincidence spectroscopies and the opportunities presented by the next generation of synchrotron radiation sources.

1. Introduction

Atomic and molecular physics has always been at the forefront of the development of the use of synchrotron radiation, and this is particularly true of the present time. Over the last few years there has been considerable progress in experimental techniques, with the result that the photoionization process can now be studied in great detail and our understanding of complex correlation phenomena has advanced considerably. This has been spurred on by the continuing improvements in synchrotron radiation sources, both in the areas of beam line optics, and machine performance in terms of beam emittance and lifetime. In particular the new third generation sources have begun to demonstrate their capabilities, setting new standards in terms of very high resolution, with unprecedented intensity.

These improvements in synchrotron radiation sources have benefited many scientific areas, and from the point of this review the one of particular

interest is that of differential measurements made with both high optical and electron resolution. In parallel with this, the efficiency of detectors has also improved, particularly in the case of electron and ion spectrometers where area detectors are now coming into widespread use. This has enabled normally weak correlation effects to be measured, either by using improved optical resolution to focus on regions where autoionization takes place, or by using the enhanced sensitivity to probe inter-channel correlations in the photoionization continuum. For molecules such measurements are of particular interest because by focussing on an autoionizing line in a molecular absorption spectrum, different vibrational levels of the ion can be populated compared to those reached by direct ionization and in those cases where the vibrational progressions are long they can provide reliable information on the molecular constants. Furthermore, measurements in resonant regions can bring to

* Research Institute for Scientific Measurements, Tohoku University

Katahira 2-1-1, Aoba-ku, Sendai 980-77

TEL 022-217-5394 FAX 022-217-5405 e-mail WEST@RISM, TOHOKU, AC. JP

Permanent address : Daresbury Laboratory, Warrington WA4 4AD, UK

light effects due to correlation between electronic and vibrational motion; this is because in the resonance region the outgoing electron is temporarily trapped and can interact with the molecular core, exchanging angular momentum with it due to anisotropic interactions. This results in marked non Franck-Condon behaviour, normally not seen in the ionization continuum, and despite considerable theoretical effort it has proved difficult in general to describe vibronic coupling quantitatively. At least in the case of small molecules, and also transient molecules whose photoionization spectra are not well known, high resolution measurements will be of continuing interest to provide both fundamental information on the excited states of the molecule and also on the vibronic coupling effects which can dominate their inner shell spectra.

Despite the experimental difficulties measurements on both singly and multiply charged ions continue to be of great interest worldwide, mainly because of their relevance to astrophysics and plasma physics. Since the first measurements on absolute cross sections were made some years ago, several laboratories worldwide are setting up experiments to extend such measurements to higher photon energies and a greater range of ions, with some success very recently. Also the first differential measurements have been made. There are now plans to extend these measurements to multiply charged ions, using improved versions of ion sources such as the Electron Cyclotron Resonance source, and these will be highly demanding experiments even for third generation storage rings. Nevertheless they are an essential complement to the Dual Laser Plasma Technique which has been used very effectively for studying the absorption spectra of multiply charged ions, and are likely to remain a significant part of synchrotron radiation based atomic physics programmes for some time to come.

It is outside the scope of this review to cover all aspects of atomic and molecular physics using synchrotron radiation, so it will focus on work done by the author and his colleagues using the synchrotron radiation source (SRS) at Daresbury Laboratory. The aim is to highlight areas which are likely to be of continuing interest for the next generation of such sources, give an indication of how these research activities in atomic and molecular physics are developing, and in what direction they are likely to proceed in future. Work in the areas of atomic double ionization, satellite structure,

excited atoms and multiple coincidence experiments applied to molecular fragmentation, which is now making an enormous contribution to the development of the subject, will therefore be included only where it is either complementary to or a natural development of the research reviewed in this article.

2. Atoms

Measurements on atoms using synchrotron radiation have of course progressed considerably from the earliest measurements of absorption spectra, reaching the point where the fundamental parameters in the photoionization process can be measured. Such experiments are often called "complete", although it should be borne in mind¹⁾ that they are complete only within the framework of the theoretical method and assumptions that are used to analyse them. Some years ago Heinzmann and his co-workers^{2,3)} made electron spectroscopy measurements on the rare gases in which the electron spin was resolved, and were able to calculate the dipole matrix elements and phase differences for the outgoing channels in the photoionization process. Jiménez-Mier et al⁴⁾ measured the angular distribution of the fluorescence resulting from the decay of He⁺ ions following photoionization to determine the alignment of the ion, and using previously measured values for the photoelectron asymmetry determined the ratio of the two dipole matrix elements and their phase difference. Hausmann et al¹⁾ carried out a similar experiment on the magnesium 2p shell, using the angular distribution of the Auger electrons to determine the ion alignment, and Kämmerling and Schmidt⁵⁾ made angular correlation measurements between the Auger and photoelectrons following ionization of xenon in its 4d shell, to determine five parameters in this relativistic case.

Calcium and Strontium

A variation on the fluorescence approach has been used in recent experiments at the Daresbury SRS, in which the polarization of the fluorescence resulting from the decay of calcium and strontium atoms⁶⁾ was measured. The experimental geometry is shown in figure 1; the experiments were carried out in the regions of the giant p-d resonances, mainly because the cross section near the threshold for ionising and exciting these atoms, where ideally this experiment should be done, was very low

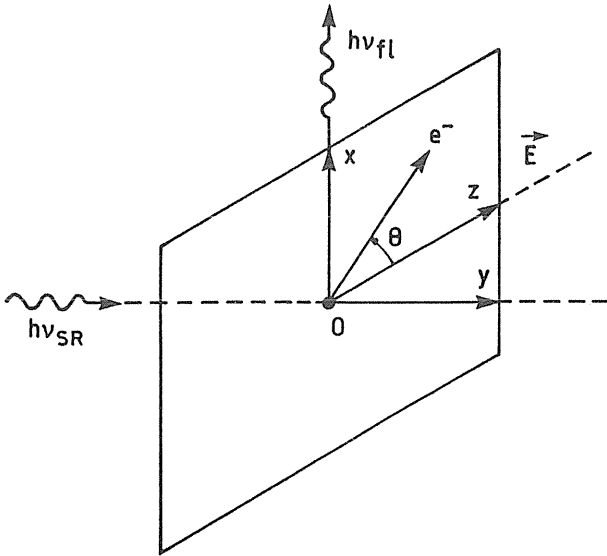


Figure 1. The experimental geometry of the electron-fluorescent photon coincidence experiment.

($\sim 10^{-19}$ cm²). When combined with measurements of the photoelectron angular distribution, for strontium reliable results for the ratio of the dipole matrix elements could be obtained at the main peak of the 4p-4d resonance, where it was shown that LS coupling could be assumed and that the effect of cascade processes feeding the fluorescing 5p level could be neglected⁷. The theoretical basis for the analysis of these results in terms of statistical tensors is well established⁸. In the case of strontium, for example, after the initial ionizing event the Sr⁺ ion is left in the ...4s²4p⁶5p²p_{1/2,3/2} levels, and decays by fluorescence to the ground state of the ion ²S_{1/2}. The measurement of the fluorescence polarization of the ²P_{3/2} → ²S_{1/2} transition gives the alignment parameter \overline{A}_{20} , and the angle resolved photoelectron measurement, on the electrons which are ejected leaving the ion in the excited 5p ²P_{3/2} level, provides the angular distribution parameter β . In LS coupling there are two outgoing continuum channels ϵs and ϵd , and the dipole matrix elements and their phase difference are related to \overline{A}_{20} and β by the following equations:

$$P = \frac{\alpha_2 \overline{3A}_{20}}{\alpha_2 \overline{A}_{20} - 2}, \text{ where } \overline{A}_{20} = \frac{|D_s|^2 + |D_d|^2 / 10}{|D_s|^2 + |D_d|^2}$$

$$\text{and } \beta = \frac{|D_d|^2 - 2\sqrt{2}|D_s||D_d|\cos\Delta}{|D_s|^2 + |D_d|^2};$$

α_2 is a geometrical factor, equal to 0.5 for a ²P_{3/2} → ²S_{1/2} transition. In order to overcome the

uncertainties due to the cascade problem, and in a new approach to the “complete” experiment, Beyer et al⁹ made coincidence measurements between the polarized fluorescent photon and the photoejected electron. The measurements were made on the calcium atom, where it was known that cascade processes could not be neglected. Again, the measurements were made in the 3p-3d resonance region, the polarized photons being detected in coincidence with the ejected electrons which leave the Ca⁺ ion in the 4p ²P_{3/2} level. The results are shown in figure 2 for two values of θ , together with values for β and the partial cross section of the 4p channel. The analysis of these experiments is now a little more complicated, since a particular angular correlation is being selected out and thus the fluorescence is no longer being averaged over all photoelectron directions. The coincidence polarization P_x is now given by

$$P_x = \frac{\alpha_2 (3A_{20} + \sqrt{6}A_{22})}{\alpha_2 (A_{20} - \sqrt{6}A_{22}) - 2}$$

where the normalized statistical tensors of the ion A_{20} and A_{22} can be expressed in terms of the incoming photon and the outgoing photoelectron. Details of this method of analysis have been given by Kabachnik¹⁰ and more recently by Kabachnik and Ueda¹¹. For $\theta = \pm 135^\circ$, the expressions simplify so that P_x is given by

$$P_x = \frac{27 - 6(R+1)(4+\beta)}{27 - 10(R+1)(4+\beta)}$$

where $R = |D_s|^2 / |D_d|^2$. Using this expression and the expression above for β , Beyer et al⁹ calculated the dipole moment ratio and phase difference Δ at the peak of the 3p-3d resonance:

$$|D_s| / |D_d| = 1.4, +0.6, -0.3$$

$$\text{and } |\Delta| = 44.2^\circ + 2^\circ, -5^\circ.$$

This applies only within the LS coupling approximation, and the justification for this came from the fact that for $\theta = 90^\circ$, the value of P_x was measured to be ~ 0.6 , as expected for LS coupling, independent of the dipole matrix elements and their relative phase¹¹. However, a further complication arises: unlike the non-coincidence measurements, the coincidence measurements are sensitive to the degree of circular polarization S_3 of the incoming

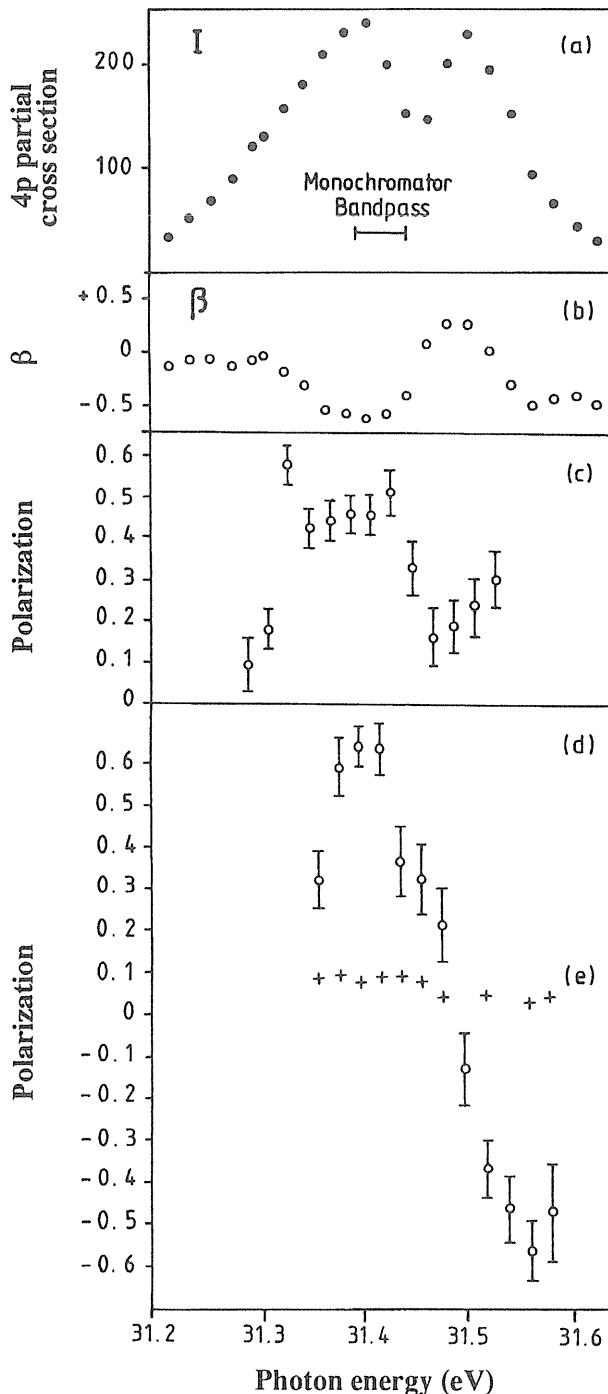


Figure 2. Experimental results in the Ca 3p-3d resonance region: (a) relative partial cross section for leaving the Ca^+ ion in the excited 4p level; (b) asymmetry parameter β for the corresponding photoelectrons; (c) polarization of the fluorescent photons, taken in coincidence with the photoelectrons, for the electron detection angle $\theta = -135^\circ$, and (d) $\theta = -90^\circ$.

light, and this was assumed to be zero when the above values were calculated. Measurements at other values of θ have to be made, other than at multiples of 90° , to provide a value of S_3 . This has recently been done with this experiment, and the

results indicate that the uncertainty in the above values for $|D_s|/|D_a|$ and $|\Delta|$ does not increase substantially.

The extension of these measurements to the non-LS coupling case is relatively straightforward, though rather demanding experimentally, since measurements over a range of θ values must be made to achieve reasonable accuracy. Further such experiments are planned for the alkaline earth atoms, with the long term goal of providing guidance to calculations of the wavefunctions used in the theoretical analysis of photoionization spectra.

Atomic ions

The majority of measurements on atoms and molecules have been made with the target in its ground state, this being the simplest to prepare with a high enough density. Nevertheless, over the last ten years there has been considerable progress in studies of photoionization of atoms in excited states, using a laser tuned to a resonance line to generate the excited state. These are limited to atoms such as the alkalis and alkaline earths where the resonance line concerned can be reached with a CW laser, since pulsed lasers and synchrotron radiation sources are in general poorly matched from the time synchronization point of view, but some benchmark measurements have been made. Dramatic changes in inner shell spectra and associated satellite intensities are seen when an outer shell electron is excited, compared to the spectra seen with the neutral atom¹²⁾. By using the laser both to align and excite the atom, angular correlation measurements have been made between the outgoing electron and the atomic alignment axis to provide detailed information on the symmetry of the states of the excited atom¹³⁾. Access to highly polarized undulator radiation has enabled considerable further progress with measurements of this kind.

The next logical step from excited atoms is to make measurements on singly charged ions, and there is considerable interest world-wide in this topic. First, it opens up the possibility of making measurements on both iso-electronic and iso-nuclear sequences, permitting observation of the ways in which phenomena, such as wavefunction collapse and intershell correlations, develop. A good example of this, for an iso-nuclear sequence, is the absorption spectra of Ba, Ba^+ and Ba^{++} measured by Lucatorto et al¹⁴⁾, in which the collective excitation of the 4d shell "moves" into the discrete

part of the spectrum¹⁵). Second, basic data on the photoionization spectra and cross sections of atomic ions are of direct relevance to solar physics and astrophysics, but to date mainly only theoretical data are available. It will be seen below, for the case of the Ca^+ ion, that theoretical analysis of the photoionization spectrum is not well advanced, and the predictive ability of modern theoretical methods is not well established for atoms of this size and larger. For this reason, and because most of the theoretical data remain untested, experimental measurements are urgently needed. There are, however, considerable experimental difficulties, with the result that progress has been slow. To begin with, the target density is generally six orders of magnitude lower for singly charged ions compared to a neutral gas target, and even worse than this for multiply charged ions because of space charge limitations. For this reason the first measurements of photoionization cross sections of atomic ions¹⁶ were made using the merged beam technique¹⁷ in which a collimated photon beam was merged with an ion beam over a length of 10 cms. Such experiments have one advantage over measurements of cross sections of neutral species: the number density of the absorbing species can be measured using counting techniques. The spatial profiles of both the photon and ion beams were measured to calculate an overlap integral; the count rates for the singly charged ions and the doubly charged ions were then measured at each photon energy. Knowing the ion velocity, the photon beam/ion beam overlap integral, the length of the region of interaction

between the two beams and the absolute value of the incident photon flux, it was possible to provide absolute cross sections. Even in this case cross sections less than 10^{-16} cm^2 could not be measured reliably, and the experiments concentrated on resonant regions where very high ($\sim 10^{-16} \text{ cm}^2$) cross sections were found.

In figure 3 the data for the p-d resonances in Ca^+ , Sr^+ and Ba^+ are shown; this is an interesting sequence because it shows the evolution of the complex structure contained within these resonances. The identity of this structure is uncertain; attempts have been made, using both the R-matrix method²¹ and the RPAE²² method to analyse the Ca spectrum, with varying degrees of success. The cross section for the 3p-3d resonance is well reproduced by both theoretical methods, but the identity of the remaining structure, particularly that due to two electron excitations, is in some doubt. Ivanov and West²² calculated the oscillator strengths for the one electron transitions and used this information to identify the most intense lines in the spectrum, confirming the earlier assignment of some of these from comparisons with the series limits calculated from the neutral atom photoabsorption spectrum²³. The weaker structure was assumed to be due to two electron excitations; by calculating the relative positions of the energy levels of these, tentative suggestions could be made for their identity.

The version of the RPAE used was the spin polarized version²⁴, in which the electrons in each subshell are split into two groups, one with spin up, the other with spin down. The individual

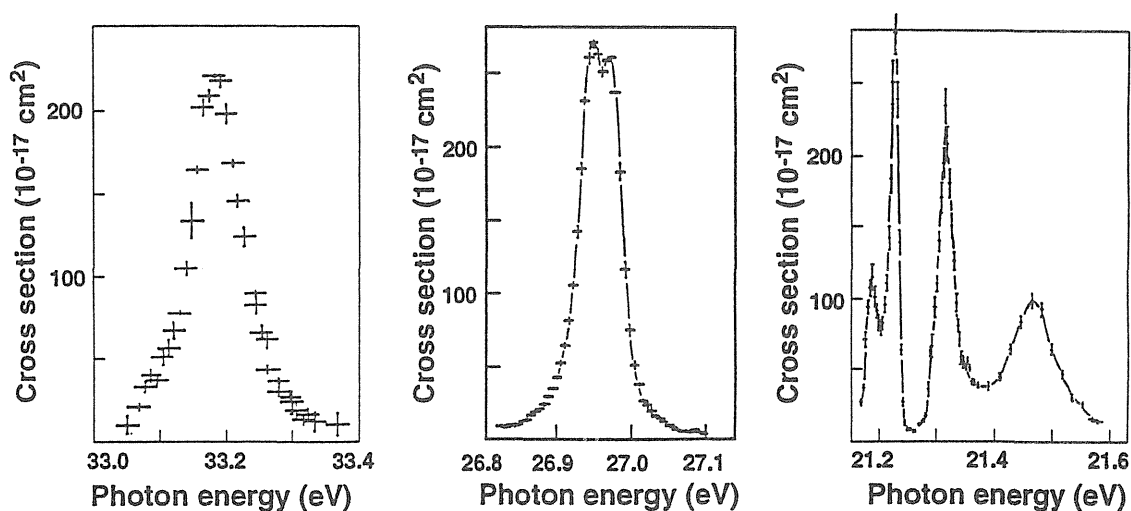


Figure 3. Total photoionization cross sections for, from left to right: the $3p \rightarrow 3d$ resonance in Ca^+ , from Ref. 18; the $4p \rightarrow 4d$ resonance in Sr^+ , from Ref. 19; the $5p \rightarrow 5d$ resonance in Ba^+ , from Ref. 20.

correlations between these electron subgroups are then calculated, to some extent simplifying the calculation since electrons with opposing spins do not interact strongly. The fact remains, however, that although the above analysis has made some progress with regard to the Ca^+ spectrum, a full theoretical analysis of this spectrum remains to be done. To this end work is proceeding to develop the RPAE method to include both the spin orbit interaction and two electron transitions²⁵⁾. On the experimental side, access to undulator radiation has encouraged new experiments on atomic ions. The first electron spectroscopy measurements on the Ca^+ ion were made in the 3p-3d resonance region by Bizeau et al²⁶⁾, and using the merged beam method Koizumi et al²⁷⁾ have extended measurements on the Ba^+ ion beyond the 4d threshold. Measurements on other ions are also under way, and the use of ECR sources for production of multiply charged ions is planned. Even the high intensity from the new third generation sources, however, does not entirely compensate for the low beam densities, and moving to higher photon energies where the cross section is lower and is partitioned into more than one ionization channel will add to the difficulties. New techniques, perhaps using coincidence methods²⁸⁾ to reduce the background problems which affect all these measurements, will be required and present a considerable challenge to the experimentalist.

3. Molecules

Although the early measurements in the gas phase using synchrotron radiation focussed on atoms, and mainly the rare gases, once the experimental techniques using the new kind of light source were established attention turned rapidly to molecular studies. Many of the phenomena, for example autoionization and shape resonances, seen in atomic photoionization, are of course seen in molecules. Shape resonances, which have their origin in the centrifugal barrier presented to electrons of high angular momentum leaving the atom and are so called because of the shape of the potential of the electron as a function of its distance from the nucleus²⁹⁾, occur widely in molecular absorption. This comes about because the outgoing electron wave contains in principle all angular momentum components, as a result of the angular momentum and spin of the individual electrons no longer being good quantum numbers and being replaced by

their projections on the molecular symmetry axis. The higher angular momentum components can therefore contribute to shape resonances, and quite complex interactions between outgoing channels can occur.

Carbon dioxide: shape resonant effects

An example of this is seen in the case of ionization of the first four electronic states of the CO_2 molecule, where shape resonances are predicted in the $\varepsilon\sigma_g$ continua of the $A^2\Pi_u$ and $B^2\Sigma_u$ states, the $\varepsilon\sigma_u$ continuum of the $X^2\Pi_g$ state and the $\varepsilon\sigma_g$ continuum of the $C^2\Sigma_g$ state, and furthermore are expected to couple with each other, through a mechanism known as continuum-continuum coupling. The measurements shown in figures 4 and 5 were taken with a high resolution electron spectrometer system³⁰⁾; although in general high resolution is not required to resolve electronic states, in the case of the CO_2 molecule the vibrational members of the A and B states overlap and high electron resolution is required to separate the contributions of these two states unambiguously. The C state shape resonance, at 42 eV photon energy, is seen quite clearly in the photoelectron angular distribution parameter corresponding to ionization to this state, shown on the left of figure 4; it is interesting to note that it does not appear in the partial cross section for this channel, shown on the right of figure 4. The same resonance is also seen in both the B state partial cross section and angular distribution parameter, shown in figure 5; no shape resonance is expected in the B state so this arises purely through coupling with the C state shape resonance. The theoretical data shown³⁷⁾ also describe the phenomenon quite well, where the single channel calculation predicts a shape resonance in the C state, but with too great a magnitude; by definition this calculation will not, of course, show the shape resonance in the other channels. The calculations for three and four coupled channels improve the agreement with experiment substantially for the C state angular distribution, and reproduce the effect in the B state quite well, showing a slight preference for the three channel calculation. The disagreement between theory and experiment for the B state cross section, where the predicted peak lies at lower energy and is much broader, remains to be resolved; it was pointed out by Lucchese³⁷⁾ that the frozen-core Hartree-Fock wave function which he used may

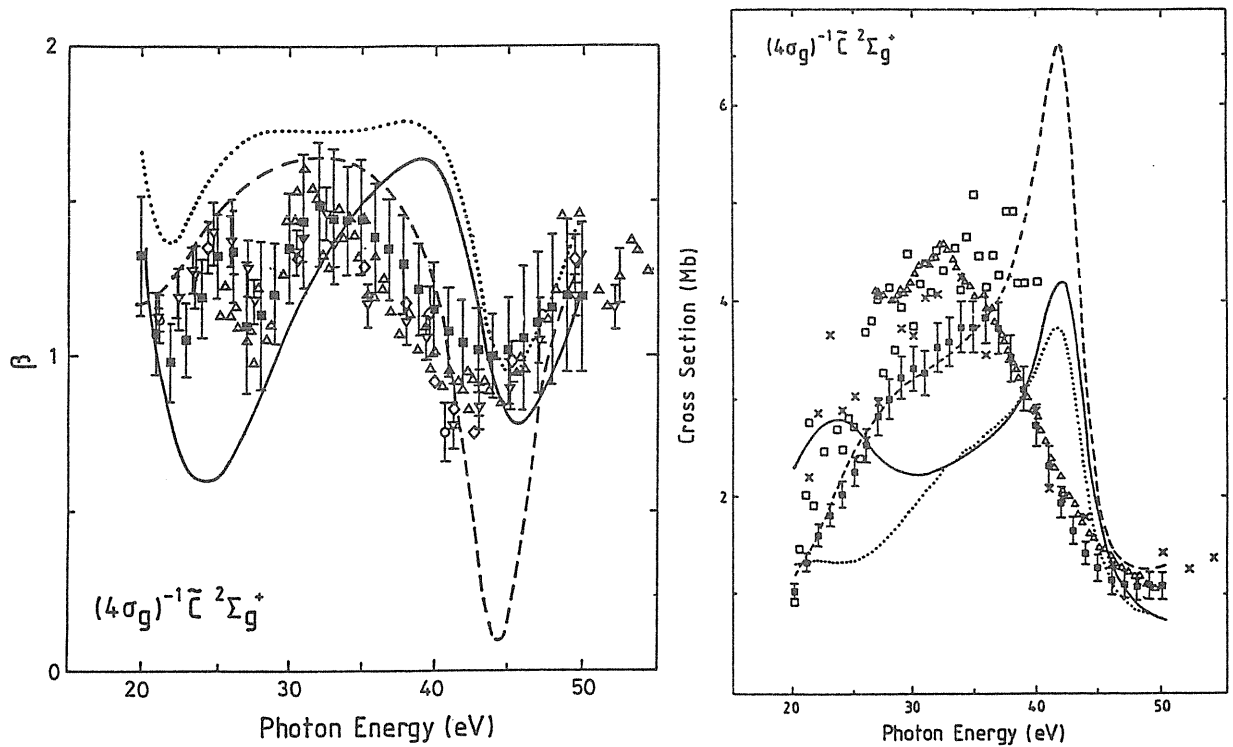


Figure 4. The angular distribution parameter β (left) and partial cross section (right) for the C state of CO_2^+ . Experimental data: \blacksquare , Ref. 31; \triangle , \diamond , Ref. 32; ∇ , Ref. 33; \circ , Ref. 34; \times , Ref. 35; \square , Ref. 36. Theoretical data from Ref. 37: ---- single channel calculation; three channel calculation; — four channel calculation.

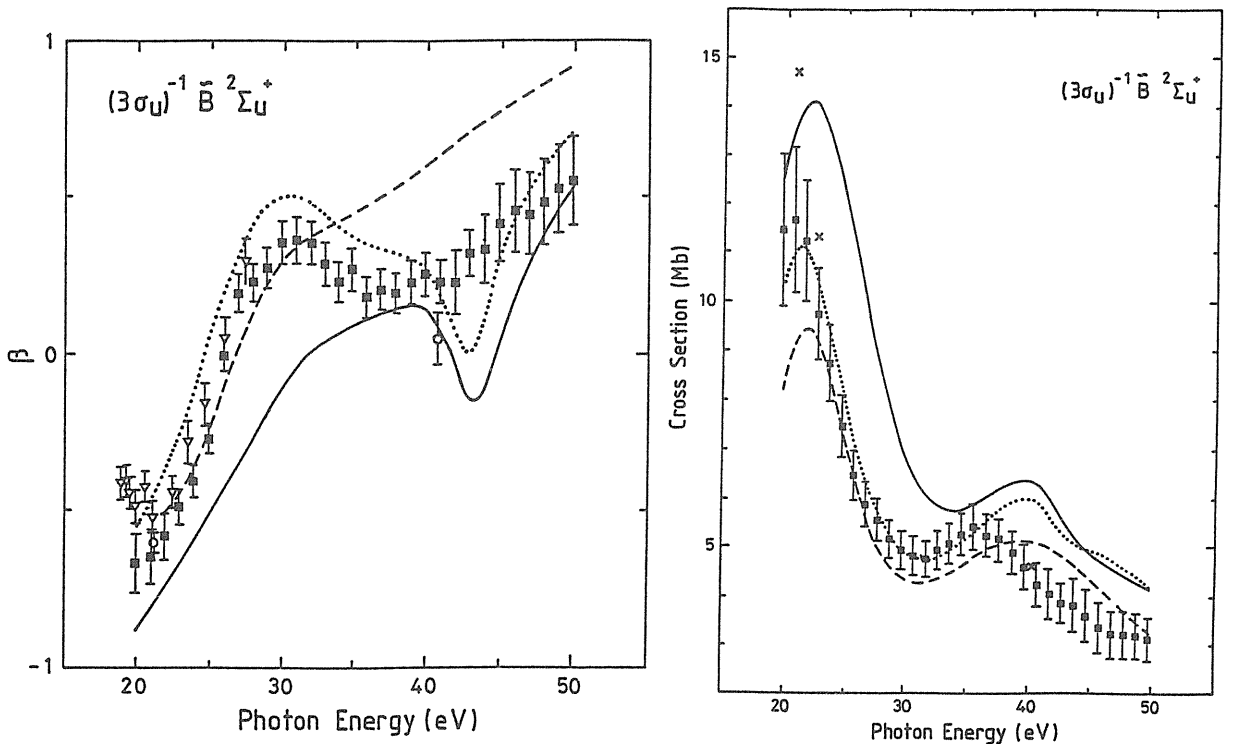


Figure 5. The angular distribution parameter β (left) and partial cross section (right) for the B state of CO_2^+ . Symbols as for Fig. 4.

not represent the ion state well, indicating that core relaxation should be included in the calculation. The coupling effects in the other channels are

examined in further detail in the experimental paper by Siggel et al³¹⁾, and two points emerge: the presence of these subtle effects can be clearly

established by the use of angle resolved electron spectroscopy, and it is necessary to measure both the complementary observables, angular distributions and partial cross sections, to bring them to

light.

Carbon dioxide: autoionization

The widespread occurrence of autoionization in

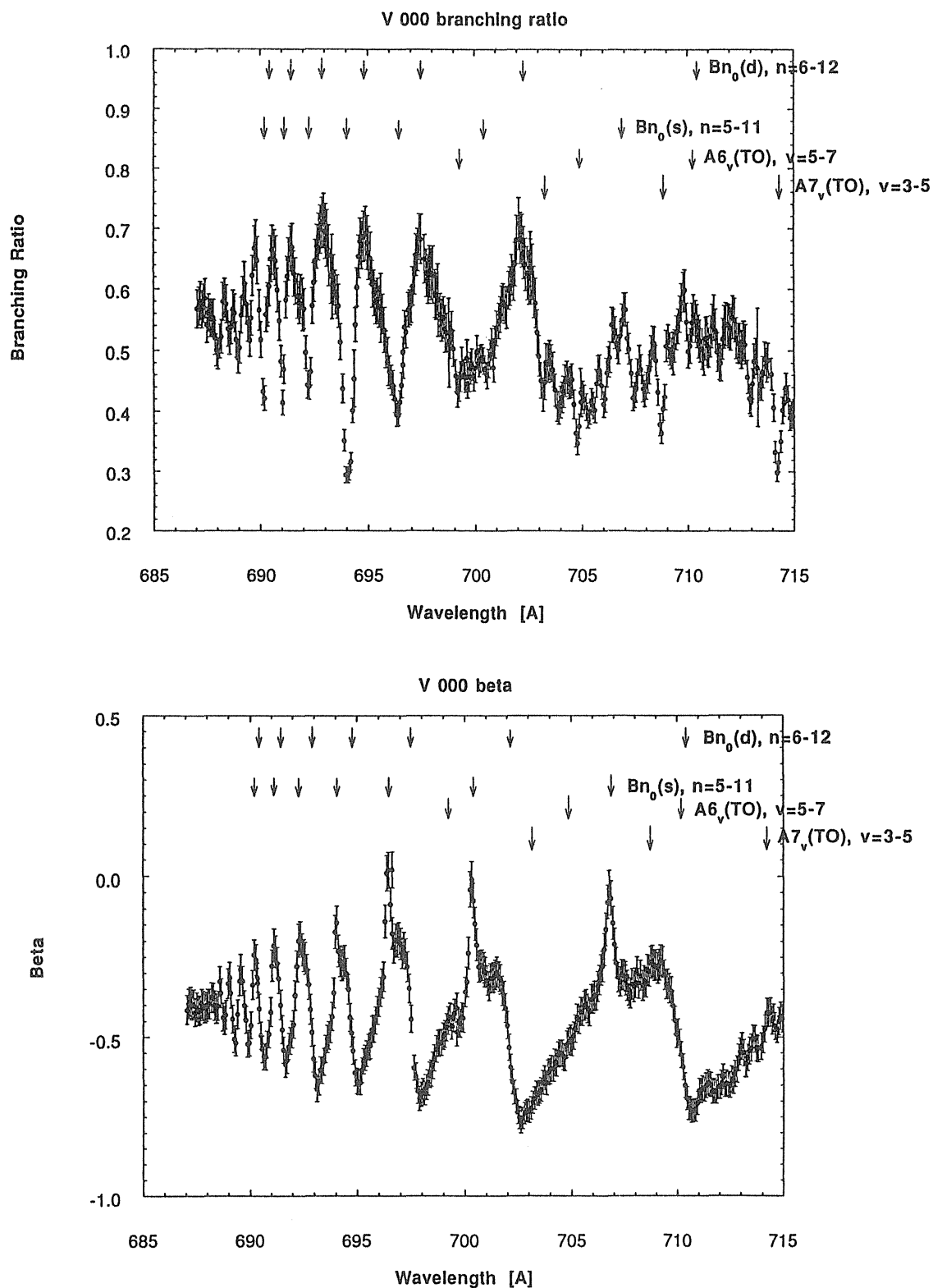


Figure 6. The relative partial cross section (upper), and β -parameter (lower), for the (000) vibrational level of the CO_2^+ ground state in the region of the Henning series.

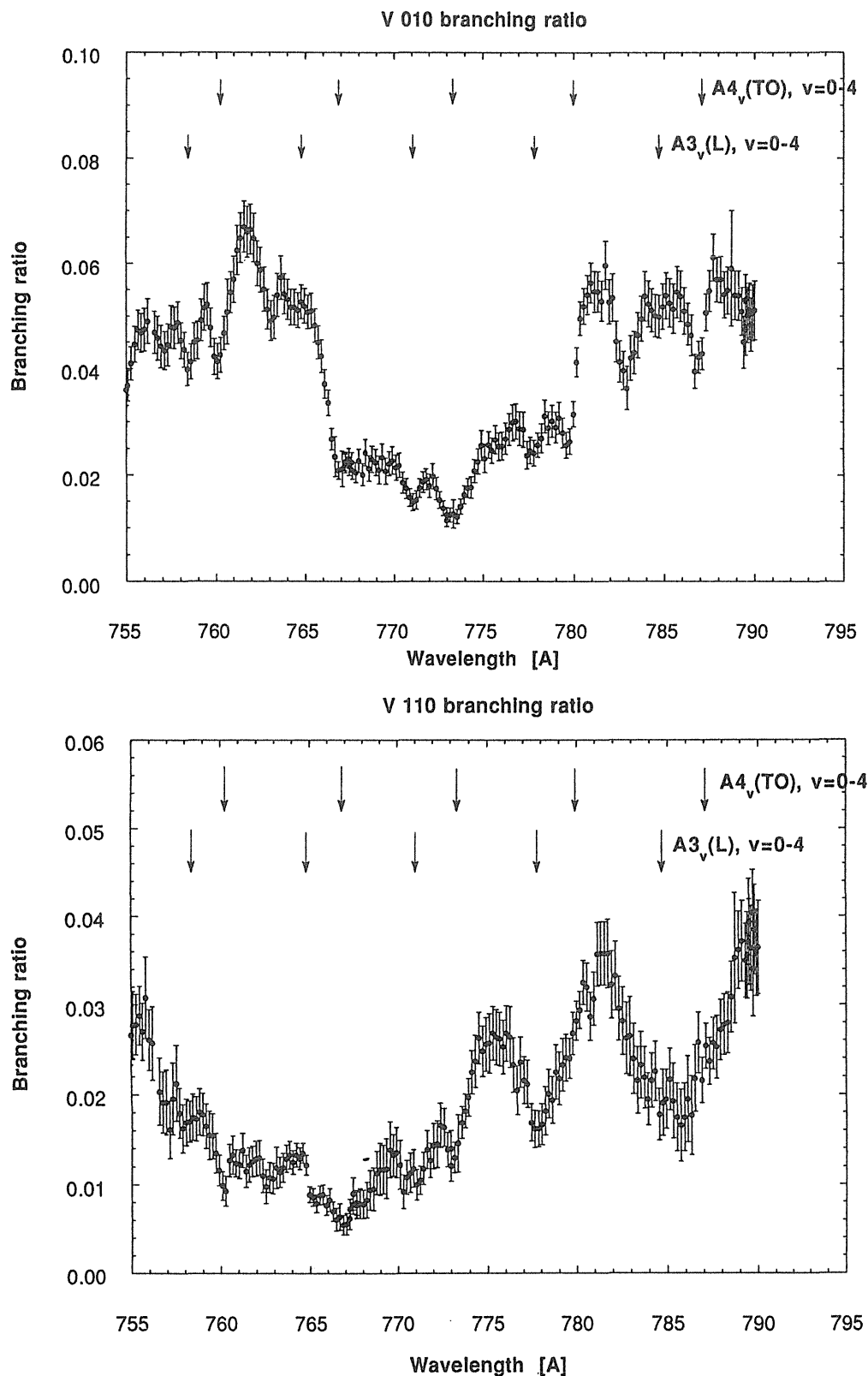


Figure 7. The relative partial cross sections of the (010) and (110) bending vibrations of CO_2^+ in the region of the Tanaka-Ogawa and Lindholm series.

molecular ionization spectra makes the analysis of the transitions involved highly complicated, especially where there are many overlapping transitions. This is particularly the case for CO_2 in the

region between the first and third ionization thresholds, where there are autoionizing series converging to both the $A^2\Pi_u$ and $B^2\Sigma_u^+$ ion states. The prominent series were identified some time ago^{38,39)},

but much of the structure remains unidentified, and there is still some doubt over the assignment of the Tanaka-Ogawa³⁸⁾ (TO) series. By using the high resolution in the photon channel provided by the 5-metre normal incidence monochromator at the Daresbury SRS⁴⁰⁾, and an electron spectrometer system with sufficient resolution and sensitivity³⁰⁾ to resolve even weak vibrational structure in the photoelectron spectrum, it has been possible to gather further information about the nature of these autoionizing series and the non Franck-Condon effects which can occur in regions of autoionization. Angular distribution parameters and branching ratios have been measured at 0.1 Å intervals from 795 Å up to the B state threshold at $\sim 687\text{Å}$ ⁴¹⁾. The first point, evident from these data, is the substantial intensity that goes into vibrational modes other than the symmetric stretch, particularly for members of the (TO) series where in some cases more than 50% of the intensity in the photoelectron spectrum goes into the bending and antisymmetric stretch vibrations. This behaviour is not reproduced at all by calculations⁴¹⁾ based on the Franck-Condon principle, particularly for members of the bending vibration with odd quantum numbers which are in principle forbidden. A sample of these data appears in figure 6, where the branching ratios and angular distribution parameters are shown for the (000) vibrational member of the CO₂⁺ ion in the region of the Henning³⁹⁾ series converging onto the B state of the ion, and in figure 7 showing the same parameters for the (010) and (110) vibrations in the region of the A_{4v} (TO) and A_{3v} (L) series members. McCulloh's⁴²⁾ notation has been used in these figures: A_{4v} (TO) means the Tanaka-Ogawa series members with the running number conventionally known as m equal to 4, vibrational quantum numbers v, converging to the A state of CO₂⁺; A_{3v} (L) refers similarly to the members of the Lindholm series⁴³⁾. In figure 6 the (s) and (d) notations refer to the Henning³⁹⁾ sharp and diffuse series respectively, converging to the B state of CO₂⁺. The relationship between the running number m and the quantum number n depends on the assignment of these series, which at present is not absolutely certain (for a full discussion see ref. 44).

By picking out just the (000) vibrational member, much more detail is evident in the spectra than is seen from a total photoionization spectrum. Particularly for the β -parameters shown in the

lower half of figure 6, the effect of interference between the sharp and diffuse members of the Henning series is seen quite clearly in the asymmetric line shapes. This pattern becomes less clear for members with low principal quantum numbers (at longer wavelengths not shown in this figure) because it is strongly overlapped by members of the Tanaka-Ogawa series converging to the various vibrational levels of the A state of the ion, but it stands out clearly for the higher members and should be amenable to theoretical analysis. In figure 7 the relative partial cross sections of the (010) vibrational members are shown in a lower incident-photon-energy region where autoionizing structure converging to the A state of the ion is prominent. It is interesting to note here that the peaks of the resonances correspond to dips in the intensities of these vibrational members, which seems counter-intuitive: the complete data set contains many further examples of this type, and a preliminary analysis is the subject of a forthcoming publication⁴¹⁾.

One explanation for this non-intuitive behaviour may lie in the contribution from the background continuum underlying the resonances, which makes any model based on the assumption of a single partial wave for the resonance inaccurate. For CO₂ this was seen quite recently in a high resolution experiment in which the spin-orbit splitting of the A state of the ion was resolved⁴⁴⁾ and the β -parameters for the two spin orbit components measured. The aim of the experiment was to examine the selectivity in populating the spin-orbit split states in resonant regions, and by measuring the β -parameter to firmly establish the assignment of the series, in this case the Tanaka-Ogawa series. A supersonic jet of CO₂ was used to reduce rotational broadening and thus resolve the splitting more clearly. The A_{5₂} resonance, the m=5, (200) member of the Tanaka-Ogawa series, was chosen and figure 8 shows a photoelectron spectrum taken at the resonance peak; the non resonant spectrum has been subtracted from this, and the data were taken at 0°, ie electrons ejected parallel to the principal polarization direction of the incoming light were analyzed. It is immediately evident that autoionization occurs primarily to the X ²Π_{1/2} state of the ion, consistent with the earlier finding by Tanaka and Ogawa³⁷⁾ that this series converges to the A ²Π_{1/2} ion core. An analysis⁴⁴⁾ of the symmetry considerations for autoionization of the Tanaka-Ogawa series, combined with the fact the quantum defects

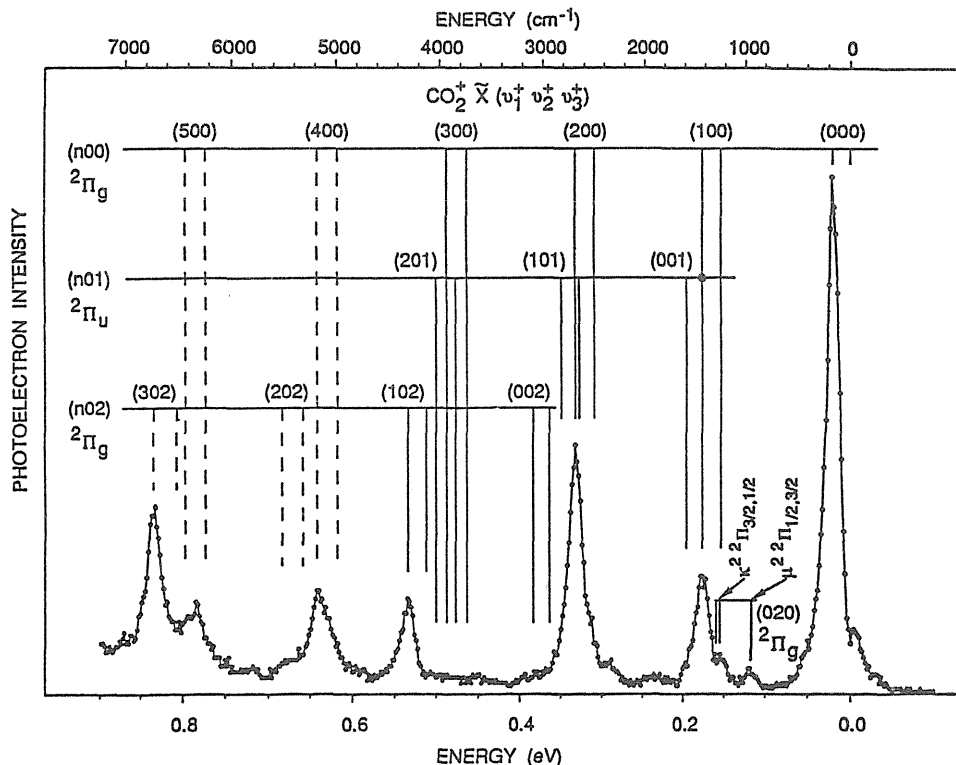


Figure 8. The photoelectron spectrum taken at the $A5_2$, $m=5$, (200) member of the Tanaka-Ogawa series. The dashed lines indicate the estimated positions of the higher vibrational members of the progressions shown. The energy scale is with respect to the $\text{CO}_2^+ \text{X} (000) {}^2\Pi_{3/2}$ level.

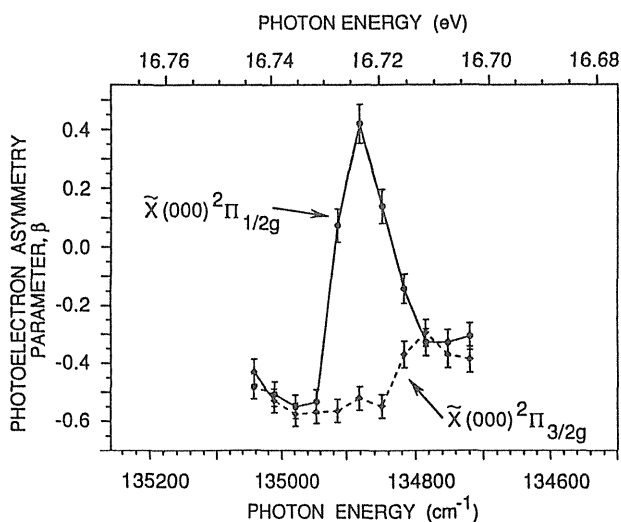


Figure 9. The photoelectron angular distribution parameters corresponding to the $\text{X} (000) {}^2\Pi_{1/2}$ and ${}^2\Pi_{3/2}$ states in the region of the $A5_2$ resonance.

are nearly constant³⁷⁾ for $m=4$ to 11, leads to the conclusion that $\Omega_c \omega$ coupling applies for this series. Also, the most likely assignment is $nd \delta_g$, which on autoionization should lead to an outgoing wave of primarily $f \delta$ symmetry, giving a β value of 0 at the peak of the resonance. Figure 9 shows a reversal of the expected behaviour, since a value greater than 0 would normally be expected

in the off resonance regions, falling to zero at the peak or possibly taking a negative value if parity unfavoured transitions⁴⁵⁾ occur through anisotropic interactions with the molecular core. Again, the reason probably lies in the contribution from the background continuum, given the weight of theoretical and quantum defect evidence for the assignment of the series as $nd \delta_g$. These measurements bring out very clearly the difficulties encountered in the analysis of these spectra, since a single partial wave analysis appears to be inadequate.

Sulphur monoxide

For diatomic molecules where there is only one vibrational mode, the analysis of the photoelectron spectra can be relatively straightforward and the presence of autoionisation in fact helpful. By focussing on an autoionising line a different region of internuclear distance is sampled, or in other words the vibrational intensities measured in the photoelectron spectrum reflect the wavefunction overlap, or Franck-Condon factors, between the autoionising level and the ion ground state. This effect was first seen, using line discharge sources, by Price⁴⁶⁾ and Natalis and Collin⁴⁷⁾ for the oxygen molecule; large differences between the HeI and

NeI photoelectron spectra occurred because by chance the NeI line coincides with an autoionizing line in the oxygen spectrum. A theoretical analysis for the case of oxygen was later carried out by Smith⁴⁸⁾, within the framework of the Franck-Condon principle. By populating more of the ion vibrational levels in this way it is possible to extract accurate values of the molecular ion vibrational constants, and the continuous spectrum provided by a synchrotron radiation source makes the method universally applicable. It has been used for the chlorine and HCl molecules^{49,50)}, and recently Dyke et al⁵¹⁾ have used it for measurements on the SO radical, in a new experiment designed to handle transient or short lived molecules. A rotatable electron spectrometer incorporating differential pumping was fitted to the 5-metre normal incidence spectrometer at the Daresbury SRS, and the SO molecule was created in a microwave discharge; further experimental details are given in the original paper⁵¹⁾. The continuum source permitted the use of the Constant Ionic State (CIS) method⁵²⁾, and this was used to advantage in this case. The results are shown in figure 10, where the photoelectron spectrometer was set at an angle of 0° to the principal polarization component of the incoming light, and on the photoelectron peaks

leaving the SO^+ ion in the $X^2\Pi$, $v^+ = 0$ or $v^+ = 2$ levels. Large differences are evident between the two spectra, reflecting the different decay probabilities of the autoionizing levels concerned. In the $v^+ = 0$ spectra vibrational progressions associated with the $a^4\Pi$ 3d and 4d states and the $A^2\Pi$ 4p and 4d states are clearly seen; the 3d series is expected to have 3d σ , π and δ components but only two of these were resolved, the second being labelled 3d'. These progressions are largely suppressed in the $v^+ = 2$ spectra, allowing the identification of peaks associated with Rydberg states converging to the SO^+ $b^4\Sigma^-$ state, using its known adiabatic ionization potential⁵³⁾.

New structure in the photoionization spectrum of SO^+ has been found in this way, extending earlier ion-electron coincidence measurements⁵⁴⁾ to energies above 12 eV. Having identified the position of the autoionising structure, the next stage was to set the incoming photon energy to coincide with an autoionising peak, and measure photoelectron spectra at resonant energies. In the case of a spectrum taken at 12.31 eV photon energy, corresponding to excitation of the seventh vibrational member of the $a^4\Pi$ 3d' autoionizing level, thirteen vibrational components were evident. Analysis of this spectrum, and several others where extensive

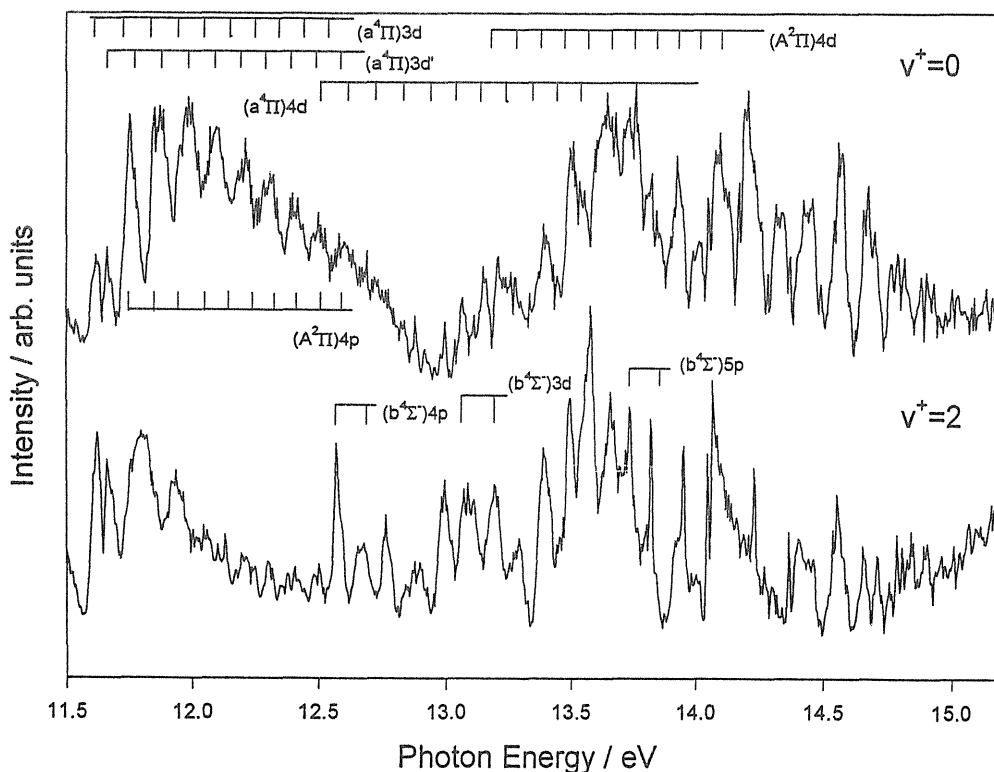


Figure 10. CIS spectra for two vibrational levels of the $\text{SO}^+ X^2\Pi$ ground state.

vibrational structure was seen, gave values of the molecular constants in good agreement with earlier determinations. The CIS measurements were then extended to photon energies above 15 eV; as seen in figure 11, Rydberg series were found which converge onto the first two vibrational levels of the $B^2\Sigma$ state of SO^+ . Two series of resonances are seen, absorption and emission types; the absorption series has a quantum defect δ of 0.12, and thus has oxygen d symmetry. The emission series was found to have $\delta = 0.52$, implying oxygen p symmetry, and the analysis of these series gave a value of 16.40 eV for the adiabatic ionisation energy of the $SO^+ \ ^2\Sigma^-$ state, consistent with, though probably more accurate than, the value obtained from earlier measurements⁵³). These preliminary measurements on the SO radical demonstrate the potential of this method; the molecular constants can be determined with high accuracy, and also, using the CIS method, partial ionization cross sections determined once the photoelectron spectra have been corrected for angular distribution effects. The angular distributions themselves will give further information on the symmetries of the orbitals concerned. Very little is known about the

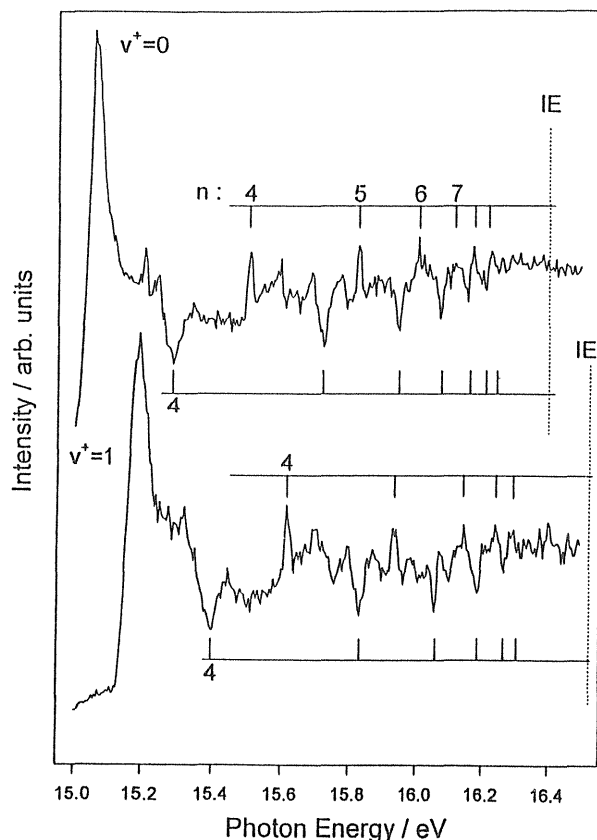


Figure 11. CIS spectra for two vibrational levels of the $SO^+ \ b \ ^4\Sigma^-$ state.

photoionization spectra of transient molecules, so the application of continuous wavelength photoelectron spectroscopy to these systems has considerable potential for the future.

4. Conclusion

The above examples have been chosen to give an idea of our understanding of the photoionization mechanism for atoms and molecules, as well as indicating directions for future progress in this area. Much of this progress will depend on the application of new techniques, made possible by the enhanced intensity now available from 3rd generation synchrotron radiation sources, and from the increasing coverage of the VUV provided by laser sources. In parallel with this, improvements in detector efficiencies have led to a considerable expansion in the use of coincidence spectroscopies. The highly correlated double ionization process has recently been studied very successfully in this way for the helium atom, where the two ejected electrons were measured in coincidence and their angular correlation also determined, first for equal energy sharing between the two electrons⁵⁵, and then for unequal sharing⁵⁶; such measurements are now being extended to other atoms⁵⁷. Their extension to double ionization of molecules, where the ion is also detected, does not seem far away. They will be greatly assisted by access to sources with a high, known content of circular polarization, recently used successfully for spin polarization measurements⁵⁸). Symmetry resolved experiments on molecules, in which, in effect, measurements are made on molecules oriented in space⁵⁹, are yielding valuable information on fragmentation pathways and have already reached a high degree of sophistication, in which both the energies and angular correlations of the ions and electrons can now be measured in a coincidence experiment⁶⁰). It seems clear that future advances in molecular photoionization will make use of the combination of the now well developed techniques of angle resolved ion, electron and fluorescence spectroscopies. Nevertheless, much remains to be done in the area of basic measurements on excited atoms, ions and short lived molecules, and high demands will be made of both the new sources and the associated experimental techniques.

5. Acknowledgments

I acknowledge with great pleasure the contribu-

tions made by my colleagues, without whom none of the work presented in this paper could have been carried out:

for the atomic fluorescence/electron coincidence work H-J Beyer and H Kleinpoppen from the University of Stirling, UK, K J Ross from the University of Southampton, UK, H Hamdy from the University of Cairo, Egypt, K Ueda from Tohoku University, Sendai, Japan and N Kabachnik from Moscow State University, Russia; for the atomic ion work I C Lyon, B Peart and K T Dolder from the University of Newcastle, UK, and V K Ivanov from St Petersburg state Technical University, Russia; for the CO₂ molecular work A C Parr from the National Institute of Standards and Technology, USA, J L and P M Dehmer from Argonne National Laboratory, M A Hayes and M R F Siggel from Daresbury Laboratory, UK and again K Ueda from Tohoku University; for the SO work J M Dyke, K Haggerston, A Morris, T G Wright and A E Wright from Southampton University, UK and S Stranges from the University of Rome: La Sapienza, Italy. Financial support for all these programmes from the Engineering and Physical Sciences Research Council, UK and partial support for the CO₂ work from the U.S. Department of Energy, Office of Energy Research, under Contract No. W-31-109-ENF-38 is also gratefully acknowledged.

References

- 1) A. Hausmann, B. Kämmerling, H. Kossmann and V. Schmidt, *Phys. Rev. Lett.* **61**, 2669 (1988)
- 2) U. Heinzmann, *J. Phys. B: At. Mol. Phys.* **13**, 3467 (1980)
- 3) Ch. Heckenkamp, F. Schäfers, G. Schönhense and U. Heinzmann, *Phys. Rev. Lett.* **52**, 421 (1984)
- 4) J. Jiménez-Mier, C. D. Caldwell and D. L. Ederer, *Phys. Rev. Lett.* **67**, 1848 (1991)
- 5) B. Kämmerling and V. Schmidt, *Phys. Rev. Lett.* **57**, 2260 (1986)
- 6) H. Hamdy, H-J. Beyer, J. B. West and H. Kleinpoppen, *J. Phys. B: At. Mol. Opt. Phys.* **24**, 4957 (1991)
- 7) K. Ueda, J. B. West, K. J. Ross, H. Hamdy, H-J. Beyer and H. Kleinpoppen, *J. Phys. B: At. Mol. Opt. Phys.* **26**, L347 (1993)
- 8) E. G. Berezhko and N. M. Kabachnik, *J. Phys. B: At. Mol. Phys.* **10**, 2467 (1977); *ibid* **12**, 2993 (1979)
- 9) H-J. Beyer, J. B. West, K. J. Ross, K. Ueda, N. M. Kabachnik, H. Hamdy and H. Kleinpoppen, *J. Phys. B: At. Mol. Opt. Phys.* **28**, L47 (1995)
- 10) N. M. Kabachnik, *J. Phys. B: At. Mol. Opt. Phys.* **25**, L389 (1992)
- 11) N. M. Kabachnik and K. Ueda, to *J. Phys. B: At. Mol. Opt. Phys.* (in press).
- 12) D. Cubaynes, J-M. Bizeau, F. J. Wuilleumier, B. Carré and F. Gounand, *Phys. Rev. Lett.* **63**, 2460 (1989)
- 13) M. Meyer, B. Müller, A. Nunnemann, T. Prescher, E. von Raven, M. Richter, M. Schmidt and P. Zimmermann, *Phys. Rev. Lett.* **59**, 2963 (1987)
- 14) T. B. Lucatorto, T. J. McIlrath, J. Sugar and S. M. Younger, *Phys. Rev. Lett.* **47**, 1124 (1981)
- 15) K. Nuroh, M. J. Stott and E. Zaremba, *Phys. Rev. Lett.* **49**, 962 (1982)
- 16) I. C. Lyon, B. Peart, J. B. West, A. E. Kingston and K. T. Dolder, *J. Phys. B: At. Mol. Phys.* **17**, 1345 (1984)
- 17) B. Peart, J. G. Stevenson and K. Dolder, *J. Phys. B: At. Mol. Phys.* **6**, 146 (1973)
- 18) I. C. Lyon, B. Peart, K. Dolder and J. B. West, *J. Phys. B: At. Mol. Phys.* **20**, 1471 (1987)
- 19) I. C. Lyon, B. Peart and K. Dolder, *J. Phys. B: At. Mol. Phys.* **20**, 1925 (1987)
- 20) I. C. Lyon, B. Peart, J. B. West and K. Dolder, *J. Phys. B: At. Mol. Phys.* **19**, 4137 (1986)
- 21) G. Miecznik, K. A. Berrington, P. G. Burke and A. Hibbert, *J. Phys. B: At. Mol. Opt. Phys.* **23**, 3305 (1990)
- 22) V. K. Ivanov and J. B. West, *J. Phys. B: At. Mol. Opt. Phys.* **26**, 2099 (1993)
- 23) M. W. D. Mansfield and G. H. Newsom, *Proc. R. Soc. A* **357**, 77 (1977)
- 24) M. Ya. Amusia, V. K. Dolmatov and V. K. Ivanov, *Sov. Phys.-JETP* **58**, 67 (1983)
- 25) V. K. Ivanov, private communication
- 26) J-M. Bizeau, D. Cubaynes, M. Richter, F. Wuilleumier, J. Obert, J-C. Puteaux, T. J. Morgan, E. Källne, S. Sorensen and A. Damany, *Phys. Rev. Lett.* **67**, 576 (1991)
- 27) T. Koizumi, Y. Itoh, M. Sano, M. Kimura, T. M. Kojima, S. Kravis, A. Matsumoto, M. Oura, T. Sekioka and Y. Awaya, *J. Phys. B: At. Mol. Opt. Phys.* **28**, 609 (1995)
- 28) M. Richter, private communication
- 29) U. Fano and J. W. Cooper, *Rev. Mod. Phys.* **40**, 441 (1968)
- 30) A. C. Parr, S. H. Southworth, J. L. Dehmer and D. M. P. Holland, *Nucl. Instrum. Methods* **222**, 221 (1984)
- 31) M. R. F. Siggel, J. B. West, M. A. Hayes, A. C. Parr, J. L. Dehmer and I. Iga, *J. Chem. Phys.* **99**, 1556 (1993)
- 32) P. Roy, I. Nenner, M-Y. Adam, J. Delwiche, M-J. Hubin-Franskin, P. Lablanquie and D. Roy, *Chem. Phys. Lett.* **109**, 607 (1984)
- 33) F. A. Grimm, J. D. Allen Jr, T. A. Carlson, M. O. Krause, D. Mehaffy, D. R. Keller and J. W. Taylor, *J. Chem. Phys.* **75**, 92 (1981)
- 34) S. Katsumata, Y. Achiba and K. Kimura, *J. Electron Spectrosc.* **17**, 229 (1979)
- 35) C. E. Brion and K. H. Tan, *Chem. Phys.* **34**, 141 (1978)

- 36) T. Gustafsson, E. W. Plummer, D. E. Eastman and W. Gudat, *Phys. Rev. A* **17**, 175 (1978)
- 37) R. R. Lucchese, *J. Chem. Phys.* **92**, 2403 (1990)
- 38) Y. Tanaka and M. Ogawa, *Can. J. Phys.* **40**, 879 (1962)
- 39) H. J. Henning, *Ann. Phys. (Leipzig)* **13**, 599 (1932)
- 40) D. M. P. Holland, J. B. West, A. A. MacDowell, I. H. Munro and A. G. Beckett, *Nucl. Instrum. Methods B* **44**, 233 (1989)
- 41) J. B. West, A. C. Parr, M. A. Hayes, P. M. Dehmer, J. L. Dehmer, M. R. F. Siggel and J. E. Hardis, to be published
- 42) K. E. McCulloh, *J. Chem. Phys.* **59**, 4250 (1973)
- 43) E. Lindholm, *Ark. Fys.* **40**, 125 (1969)
- 44) A. C. Parr, P. M. Dehmer, J. L. Dehmer, K. Ueda, J. B. West, M. R. F. Siggel and M. A. Hayes, *J. Chem. Phys.* **100**, 8767 (1994)
- 45) D. Dill and U. Fano, *Phys. Rev. Lett.* **29**, 1203 (1972); D. Dill, *Phys. Rev. A* **7**, 1976 (1973)
- 46) W. C. Price, *Molecular Spectroscopy*, ed P. Hepple (Institute of Petroleum, London, 1968) p221
- 47) P. Natalis and J. E. Collin, *Chem. Phys. Lett.* **2**, 414 (1968)
- 48) A. L. Smith, *J. Quant. Spectrosc. Radiat. Transfer*, **10**, 1129 (1970)
- 49) T. Reddish, A. A. Cafolla and J. Comer, *Chem. Phys.* **120**, 149 (1988)
- 50) A. A. Cafolla, J. Comer and T. Reddish, *J. Phys. B: At. Mol. Opt. Phys.* **21**, 3571 (1988)
- 51) J. M. Dyke, D. Haggerston, A. Morris, S. Stranges, J. B. West, T. G. Wright and A. E. Wright, *J. Elec. Spec. Rel. Phen.* (in press)
- 52) G. J. Lapeyre, J. Anderson, P. L. Gobby and J. A. Knapp, *Phys. Rev. Letts.* **33**, 1290 (1974)
- 53) J. M. Dyke, L. Golob, N. Jonathan, A. Morris and M. Okuda, *J. Chem. Soc. Faraday Trans. II* **70**, 1818 (1974)
- 54) K. Norwood and C-Y Ng, *Chem. Phys. Letts.* **156**, 145 (1989)
- 55) A. Huetz, P. Lablanquie, L. Andric, P. Selles and J. Mazeau, *J. Phys. B: At. Mol. Opt. Phys.* **27**, L13 (1994)
- 56) O. Schwarzkopf, B. Krässig, V. Schmidt, F. Maulbetsch and J. S. Briggs, *J. Phys. B: At. Mol. Opt. Phys.* **27**, L347 (1994)
- 57) S. J. Schaphorst, B. Krässig, O. Schwarzkopf, N. Scherer and V. Schmidt, *J. Phys. B: At. Mol. Opt. Phys.* **28**, L233 (1995)
- 58) N. B. Brookes, G. Snell, M. Drescher, N. Müller, U. Heinzmann, F. Heiser, U. Hergenbahn, J. Viehhaus, R. Hentges, O. Gessner and U. Becker, *ESRF Newsletter No 24*, 17 (1995)
- 59) E. Shigemasa, J. Adachi, M. Oura and A. Yagishita, *Phys. Rev. Letts.* **74**, 359 (1995)
- 60) K. Ueda, K. Ohmori, M. Okunishi, H. Chiba, Y. Sato, T. Hayaishi, E. Shigemasa and A. Yagishita, *Phys. Rev. A* **52**, R1815 (1995).